Rationally designed anti-HER2/neu peptide mimetic disables P185$^{HER2/neu}$ tyrosine kinases in vitro and in vivo

Byeong-Woo Park[1†], Hong-Tao Zhang[1†], Chuanjin Wu[1†], Alan Berezov[1], Xin Zhang[1], Raj Dua[2], Qiang Wang[1], Gary Kao[3], Donald M. O'Rourke[1,4], Mark I. Greene[1*], and Ramachandran Murali[1*]

[1]Department of Pathology and Laboratory Medicine, Center for Receptor Biology and Cell Growth, University of Pennsylvania School of Medicine, 36th and Hamilton Walk, Philadelphia, PA 19104. [2]Xcyte Therapeutics, Inc., Seattle, WA, 98122. [3]Department of Radiation Oncology, University of Pennsylvania School of Medicine, 36th and Hamilton Walk, Philadelphia, PA 19104. [4]Department of Neurosurgery, University of Pennsylvania School of Medicine, 36th and Hamilton Walk, Philadelphia, PA 19104. *Corresponding authors R.M. (murali@xray.med.upenn.edu) or M.I.G. (greene@reo.med.upenn.edu). †These authors contributed equally to this work.

Received 29 July 1999; accepted 14 December 1999

Monoclonal antibodies specific for the p185$^{HER2/neu}$ growth factor receptor represent a significant advance in receptor-based therapy for p185$^{HER2/neu}$-expressing human cancers. We have used a structure-based approach to develop a small (1.5 kDa) exocyclic anti-HER2/neu peptide mimic (AHNP) functionally similar to an anti-p185$^{HER2/neu}$ monoclonal antibody, 4D5 (Herceptin). The AHNP mimetic specifically binds to p185$^{HER2/neu}$ with high affinity (K_D = 300 nM). This results in inhibition of proliferation of p185$^{HER2/neu}$-overexpressing tumor cells, and inhibition of colony formation in vitro and growth of p185$^{HER2/neu}$-expressing tumors in athymic mice. In addition, the mimetic sensitizes the tumor cells to apoptosis when used in conjunction with ionizing radiation or chemotherapeutic agents. A comparison of the molar quantities of the Herceptin antibody and the AHNP mimetic required for inhibiting cell growth and anchorage-independent growth showed generally similar activities. The structure-based derivation of the AHNP represents a novel strategy for the design of receptor-specific tumor therapies.

Key Words: ErbB2, Her2, neu, mimetic, doxorubicin, Herceptin, γ-radiation, tumor therapy

The p185$^{HER2/neu}$ (also called c-erbB-2) oncoprotein is the human analog of p185^{neu} and is overexpressed in ~25–35% of human breast, ovarian, and colon cancers[1,2]. Monoclonal antibodies to the ectodomain of p185^{neu}[3,4] and to p185$^{HER2/neu}$ (Herceptin)[5] have been shown to be effective in limiting growth of tumors in vivo. Recombinant humanized anti-HER2 monoclonal antibody[5] rhuMAb4D5 (Herceptin)[6–8] was developed as a useful anti-oncoprotein therapeutic agent based on earlier observations by Drebin and colleagues[4,9,10], showing that anti-p185^{neu} ectodomain specific antibodies reverse the malignant phenotype in vitro and in vivo.

The use of full-length monoclonal antibodies in clinical applications may be limited by: (1) the difficulty or expense of commercial-scale production (2) exclusion of monoclonal antibody from compartments such as the blood/brain barrier (3) limited ability for monoclonal antibodies to penetrate cells and tissues[11], and (4) the possibility of severe side effects such as induction of anti-idiotypic antibodies and immune complex formation.

In instances when only a defined surface of the protein mediates activity, smaller peptides represent obvious alternatives as mimics for larger macromolecular structures. Although peptide mimetics themselves are seldom used as therapeutic agents, they can be used as a template and through iterative reductions in size and increases in biological activity may lead to viable therapeutic reagents[12–17] better suited for clinical application than full-length antibody.

We have developed a structure-based procedure for designing peptidomimetics that focuses on small loops and turn reversals of members of the immunoglobulin gene family[18–20]. Using this method we have designed a 1.5 kDa anti-p185$^{HER2/neu}$ peptidomimetic, AHNP, that is comparable in potency to the full-length monoclonal antibody and exhibits biochemical and biological properties that are predictive of therapeutic use. The general approach described here may be considered a paradigm for development of specific receptor-based therapies, and AHNP may be considered a viable candidate for use in clinical trials aimed to treat p185$^{HER2/neu}$-positive human cancers.

Results and discussion

Structure of the AHNP. Structural studies of several antigen–antibody complexes have shown that of the six variable loops[21], the heavy-chain CDR3 loop often, but not always, mediates most of the contact with antigen[22,23]. Furthermore, they show that antibodies can provide a structural internal image of a given antigen[24]. Based on these observations, we have designed mimetics derived from CDR3 loops of anti-p185$^{HER2/neu}$ monoclonal antibodies.

We analyzed CDR loops from the deduced structure of the monoclonal antibody 7.16.4 (M.I.G. and P. Alzari, unpublished results) and the crystal structure of rhuMab4D5[7,5,16]. Both monoclonal antibodies 7.16.4 and rhuMAb4D5 seem to bind to an overlapping epitope on the p185$^{HER2/neu}$ ectodomain[27]. The CDR3H loop of both antibodies showed 41% similarity in their primary structure, and molecular modeling revealed the predicted folding of these loops to be similar. Therefore we used heavy-chain CDR3 loops of rhuMAb4D5 and 7.16.4 as templates to design several analogs, using strategies developed earlier[15,19,20,28]. The analogs were then tested for their biological activity. Mimetics that showed activity higher than 200 μM were considered minimally active in cell growth inhibition assays and ignored (data not shown).

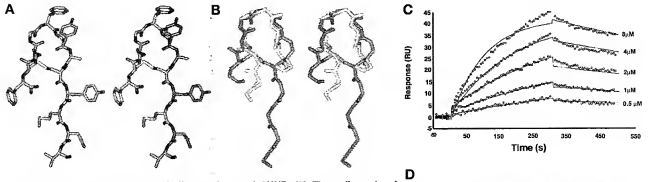

Figure 1. Structural and kinetic binding analyses of AHNP. (A) Three-dimensional structure of AHNP from molecular modeling is shown in stereo. AHNP adopts the β-turn conformation similar to the anti-p185$^{Her2/neu}$ antibody. The extending hydrophobic tail shows a β-sheet-like extended structure similar to that adopted by the framework region of an antibody. These residues were included to enhance the surface area of the AHNP. (B) AHNP is compared with the conformation of CDR3 loop of the antibody (1FVD ; ref. 25). The backbone structures of CDR3 loop of 1FVD (yellow) and the AHNP (red) are very similar and, when superimposed onto each other, the CDR3 loops differ by only 2.2 Å for Cα atoms. (C) Kinetic binding of AHNP and rhuMab4D5 to p185$^{Her2/neu}$ receptor is shown. (C) AHNP and (D) rhuMab4D5 bind in a dose dependent manner to p185$^{Her2/neu}$ receptor. The association and dissociation of AHNP and rhuMab4D5 were studied at different concentrations. AHNP at concentrations of 0.5, 1.0, 2.0, 4.0 μM were injected over a surface containing 3,600 RU of p185$^{HER2/neu}$. At 300 s, the sample was replaced with buffer, and dissociation followed for 3 min. The measured binding affinity of AHNP (K_d) is 300 nM compared to K_d of 1 nM for Herceptin.

Analysis of several analogs has shown that two structural features of the peptides seem to affect potency of cyclic peptides: (1) ring size and (2) inherent flexibility[29,30]. Residues at the C terminus also seemed critical for activity. To enhance stability, folding, and avidity, we employed aromatic modification[15,31,32]. To extend the surface area at the interface of interaction, we used extended residues (MDV) beyond the stabilizing cysteine residues in all of the AHNP species.

One of the compounds (FCGDGFYACYMDV) showed moderate activity at IC_{50} of 100 μM. High-pressure liquid chromatography (HPLC) analysis of this mimic revealed two predominant forms of the peptides, and one species had higher activity (data not shown). Upon sequencing, it was noted that the Gly3 was missing. A model without Gly3 revealed a more classical β-turn (Fig. 1A) than the original peptide. The putative contact residues of these peptide mimetics seem to have a similar relative disposition (root mean square deviation for Cα atoms is 2.2 Å) to that of the CDR3H of the parent antibody rhuMAb4D5 (Fig. 1B). Thus, exocyclic peptides that adopt rigid (compared to the original peptide mimic with extra glycine) and comparable ring sizes to β-turns may be capable of high-affinity binding activity.

Kinetic binding affinity of AHNP. Anti-HER 2/neu peptide has a 300 nM binding affinity for the p185$^{HER2/neu}$ (Fig. 1C). Based on the association and dissociation kinetics using a 1:1 Langmuir model for simple bimolecular interactions, the affinity of AHNP was shown to

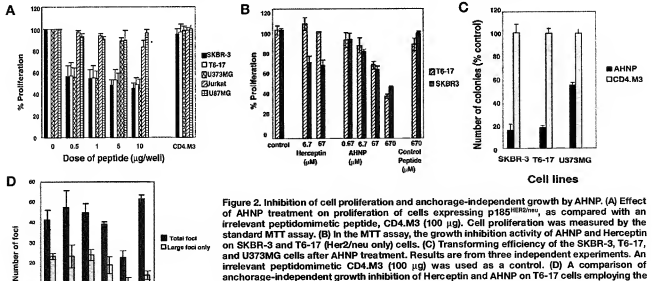

Figure 2. Inhibition of cell proliferation and anchorage-independent growth by AHNP. (A) Effect of AHNP treatment on proliferation of cells expressing p185$^{HER2/neu}$, as compared with an irrelevant peptidomimetic peptide, CD4.M3 (100 μg). Cell proliferation was measured by the standard MTT assay. (B) In the MTT assay, the growth inhibition activity of AHNP and Herceptin on SKBR-3 and T6-17 (Her2/neu only) cells. (C) Transforming efficiency of the SKBR-3, T6-17, and U373MG cells after AHNP treatment. Results are from three independent experiments. An irrelevant peptidomimetic CD4.M3 (100 μg) was used as a control. (D) A comparison of anchorage-independent growth inhibition of Herceptin and AHNP on T6-17 cells employing the focus formation assay as described in the Experimental protocol.

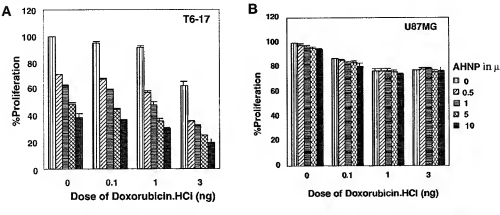

Figure 3. Combined cytotoxicity of doxorubicin and AHNP. The antiproliferation effect of doxorubicin HCl as determined by dose-dependent administration of AHNP (A) in human p185$^{HER2/neu}$-positive T6-17 cells (B) and in human U87MG cells expressing negligible concentrations of p185$^{HER2/neu}$. Results represent the mean ± s.e. of three readings.

have a K_D of 3.59×10^{-7} M. The apparent k_{on} and k_{off} rate constants were estimated to be $1.32 \times 10^5\ M^{-1}\ s^{-1}$ and $4.74 \times 10^{-4}\ M^{-1}\ s^{-1}$, respectively. Based on a bivalent model, the monoclonal antibody rhuMAb4D5 binds the p185$^{HER2/neu}$ receptor with a K_D of 1.04×10^{-9} M with k_{on} and k_{off} $1.18 \times 10^5\ M^{-1}\ s^{-1}$ and $1.23 \times 10^{-4}\ M^{-1}\ s^{-1}$, respectively.

The k_{off} value is considered as critical for kinetic binding in the development of therapeutics of biological activity[35,36] and generally correlates with potent biological effects[35]. Although the K_D of the AHNP species binds with less affinity than that of the monoclonal antibody, their k_{off} rate is very similar, which suggests that the AHNP forms a stable receptor complex. High-pressure liquid chromatography studies revealed AHNP existed as a monomer only (data not shown).

To assess the specificity of this interaction, the tumor necrosis factor receptor-(ectodomain)-Fc (TNFR-Fc) receptor was immobilized to the sensor surface. The AHNP did not bind to TNFR-Fc, indicating that AHNP polypeptide is specific for the p185$^{HER2/neu}$ ectodomain (data not shown). Calculated and experimentally observed maximum binding capacities of the commercially produced rhuMAb4D5 were comparable (Fig. 1D). No interaction of the peptide with the matrix was observed (data not shown).

Downmodulation of surface p185$^{HER2/neu}$ receptors by AHNP. Downmodulation of p185$^{her2/neu}$ by AHNP was modest (only about 25% of total surface receptors downmodulated) and far less than with monoclonal antibody 7.16.4 treatment of p185^{neu}-expressing cells (data not shown)[36]. Mechanisms involved in downmodulation of type 1 receptor tyrosine kinase (RTKs) of the erbB family of receptors have not been completely defined. Efficient downmodulation of erbB receptor kinases apparently requires an intact tyrosine kinase activity as well as a structural module within the C terminus[37]. Because AHNP is able to downmodulate surface p185$^{HER2/neu}$ receptors to a smaller extent than the monoclonal antibody, downmodulation may be driven by induced conformational changes in the receptor, and this allosteric effect may trigger other inhibitory signals, which then affect phenotype.

AHNP inhibits cell proliferation and anchorage-independent growth. We analyzed the growth characteristics of peptidomimetic-treated cells using the MTT (3-(4,5-dimethylthiazol-2-yl)-2,5-diphenyltetrazolium bromide) assay for mitochondrial viability[38] in an adherent-cell assay. In three cell lines overexpressing p185$^{HER2/neu}$ at various concentrations, treatment with AHNP resulted in 33–53% inhibition of cell proliferation (Fig. 2A). The dose-dependent inhibition is best seen in Figure 2B. Adherent-cell proliferation was unaffected by AHNP or CD4.M3 treatment in Jurkat and U87MG cells that do not contain p185$^{HER2/neu}$ (Fig. 2A). These data suggest that AHNP, such as anti-p185$^{HER2/neu}$ antibodies[8,19], specifically inhibits proliferation of p185$^{HER2/neu}$-expressing cells. As seen in Figure 2B, we conducted a comparison of the molar amounts of the Herceptin antibody and AHNP required to affect the growth of cells that overexpress p185$^{HER2/neu}$ (T6-17) or that overexpress p185$^{HER2/neu}$ and EGFr (SKBR-3). Anti-HER 2/neu peptide was better at inhibiting T6-17 growth and equivalent to Herceptin at inhibiting SKBR-3 growth.

Inhibition of cell transformation was assessed using an anchorage-independent growth focus formation assay. The AHNP treatment of cells from three transformed lines inhibited the development of morphologically transformed foci (Fig. 2C). Transforming efficiencies of SKBR-3, T6-17, and U373MG cells were inhibited 84.1 ± 5.6% (mean ± s.e.m.), 81.9 ± 1.8%, and 44.2 ± 1.6%, respectively, by AHNP treatment in three independent experiments. However, treatment with an irrelevant mimetic, CD4.M3, did not result in any inhibition of transforming efficiency of the same cell lines (Fig. 2C). A comparison of Herceptin and AHNP revealed that Herceptin was slightly better at inhibiting large foci formation of T6-17 cells but less efficient than AHNP at inhibition of all sized foci (Fig. 2D).

Enhanced inhibition of cell proliferation by doxorubicin with cotreatment with AHNP. Treatment with AHNP increased doxorubicin-mediated inhibition of cell proliferation in p185$^{her2/neu}$-overexpressing T6-17 cells (Fig. 3A). With doxorubicin alone at a dose of 3 nM, minimal inhibition of cell growth (40%) was observed. Cotreatment with AHNP resulted in additive and possibly synergistic inhibition at 5–10 µM, whereas 0.5–1 µM of AHNP resulted in inhibition that was additive with doxorubicin effects (Fig. 3A).

Anti-HER 2/neu peptide-mediated inhibition was observed at all doses of doxorubicin. However, AHNP treatment did not enhance the inhibition of cellular proliferation of U87MG cells that do not contain

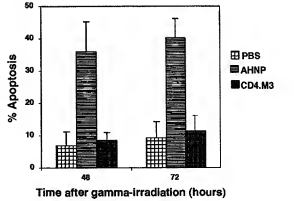

Figure 4. AHNP enhances γ-irradiation-induced apoptosis. Enhanced apoptotic cell death observed at 48 h and 72 h following γ-irradiation, after pretreatment of p185$^{HER2/neu}$-positive U373MG human astrocytoma cells with AHNP. Cells were pretreated with either PBS or a similar amount of an irrelevant peptidomimetic of identical molecular mass (CD4-M3) as controls.

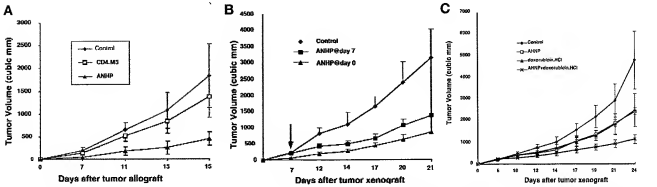

Figure 5. Inhibition of in vivo tumor growth by administration of AHNP. Tumor growth mediated by T6-17 cells was assessed in athymic mice. (A) Mice were administered 200 μg of AHNP, the irrelevant mimetic CD4.M3, or PBS by intraperitoneal injection, three times weekly beginning on the day of T6-17 cell inoculation. (B) Same experiments as in (A), except that AHNP was given to mice on the day of inoculation (AHNP@day 1) or seven days after (AHNP@day 7). (C) The effect of cotreatment with AHNP on the antitumor activity of doxorubicin against well-established T6-17 tumor xenografts. Results are given as mean tumor volume ± s.e. Tumor growth in animals treated with both reagents was significantly ($P < 0.001$) different compared to controls.

$p185^{HER2/neu}$ (Fig. 3B). U87MG cells exhibited only 20–25% inhibition of cell growth at doses of 3 nM doxorubicin. U87MG cells lack $p185^{her2/neu}$ and contain elevated concentrations of endogenous epidermal growth factor receptor (EGFR)[40], in addition to low concentrations of erbB3 and erbB4 proteins (data not shown). These data indicate that AHNP selectively inhibits proliferation of $p185^{HER2/neu}$-expressing cells in which p185 is contributing to the transformed phenotype.

AHNP increases tumor cell death in response to γ-irradiation. Induction of apoptosis rather than cell cycle arrest may underlie successful anticancer treatment[40,41]. Therefore we examined whether AHNP could enhance cell death induced by radiation.

Incubation with AHNP of U373MG cells containing elevated EGFR concentrations and moderately elevated concentrations of $p185^{HER2/neu}$ followed by γ-irradiation resulted in 36% and 40% cell death at 48 h and 72 h, respectively, compared to cell death fractions of about 10% observed at all time points in untreated U373MG cells (Fig. 4). As a control, an irrelevant peptide mimetic of equivalent molecular mass, CD4.M3, was shown to not enhance radiation-induced apoptosis.

Inhibition of in vivo tumor growth by AHNP. Small exocyclic peptides have short half-lives and may be cleared before they can induce biological changes. However, we have found that AHNP is an active molecule in in vivo assays. In an athymic mouse model, monoclonal antibody 4D5 was shown to localize at the site of tumors in vivo and inhibit the growth of human tumor xenografts that overexpress $p185^{HER2}$/neu (ref. 39).

In vivo growth of T6-17 transfected fibroblasts expressing human $p185^{her2/neu}$ was evaluated in athymic mice. In the first set of studies, AHNP was administered intraperitoneally three times weekly following inoculation of tumor cells in the flank. Sustained treatment with AHNP resulted in inhibition of tumor xenograft formation. Administration of a size-matched irrelevant peptidomimetic peptide, CD4.M3, or phosphate-buffered saline (PBS) had no effect on tumor growth (Fig. 5A). We then AHNP administered intraperitoneally after the development of small palpable tumors derived from the T6-17 fibroblast. AHNP also inhibited progression of tumor formation in these animals, indicating that AHNP could inhibit progression of growth of established tumors (Fig. 5B).

As with studies using the full-length rhuMAb4D5 in our hands, growth delay alone was observed because tumors eventually grew in all treated animals. This result suggests that the action of the AHNP is cytostatic, and not cytotoxic, a feature described in previous reports using full-length antireceptor antibodies[10,42].

Inhibition of in vivo tumor growth is enhanced by coadministration of doxorubicin and AHNP. Although AHNP and doxorubicin independently showed inhibition of established tumor growth, administration of both AHNP and doxorubicin increased growth inhibition of tumor xenografts in an additive manner (Fig 5C). Similar concentrations of inhibition were observed in vivo with either AHNP or doxorubicin. Inhibition of tumor cell growth in vivo by treatment of U373MG cells with AHNP alone revealed that the AHNP could inhibit tumor growth in cells expressing $p185^{HER2/neu}$ in combination with EGFR and other erbB proteins (data not shown).

In summary, we have reduced the macromolecular structure of a monoclonal antibody to a small secondary structure mimetic that has high affinity and in vivo activity against tumor growth, creating a true "antibody mimic." This small molecule has comparable affinity and molar activities as the parental Herceptin antibody. Creation of such small antibody mimics not only eliminates the laborious humanization of antibodies, but also provides a new avenue in the design of antibody-based therapy.

Experimental protocol

Design of AHNP. We analyzed the crystal structure of anti-$p185^{HER2/neu}$ receptor antibody (1FVD[25,28]) and the structural model of an anti-$p185^{neu}$ antibody (7.16.4) that binds rodent and human p185 and compared all of the CDRs of both monoclonals for sequence and structural similarity using a variety of software including BLAST, CLUSTALW, and AbM (Oxford Molecular, Mountain View, CA). Details of the procedure in the design of peptidomimetic are described in Takasaki and coworkers[30]. Molecular modeling and the structural analyses were carried out using both QUANTA and INSIGHT (Molecular Simulation, San Diego, CA).

Kinetic binding analysis. Biosensor experiments were carried out on both Biacore X and Biacore 2000 (Biacore AG, Uppsala, Sweden) instruments at 25°C. Recombinant purified $p185^{HER2/neu}$ receptors composed of the ectodomain of $p185^{HER2/neu}$ fused to the Fc of human IgG (provided by Dr. Che Law, Xcyte Therapeutics, Seattle, WA) were immobilized to the dextran hydrogel on the sensor surface (Biacore CM5 sensor chip) with a surface density of 3,600 resonance units (RU). Surface plasmon resonance (SPR) measurements were carried out under a continuous flow of 20 ml^{-1} min^{-1}. The surface was regenerated to remove all bound analyte among binding cycles using a mixture of organic solvents composed of dimethyl sulfoxide (DMSO), acetonitrile, 1-butanol, formamide, and ethanol, each at 0.2% (v/v) concentration in water. The apparent rate constants (k_{on} and k_{off}) and the equilibrium-binding constant (K_D) for the receptor–peptide binding interaction were estimated from the kinetic analysis of sensorgrams, using the BIA evaluation 3.0 software (Biacore International AB, Uppsala, Sweden).

Cell lines. We used several human tumor cells expressing variable concentrations of $p185^{HER2/neu}$ receptors all of which we characterized for $p185^{HER2/neu}$ concentrations by flow cytometric analysis and quantitative immunoprecipitation: (a) U87MG cells and Jurkat cells (negligible $p185^{HER2/neu}$) (b) U373MG cells expressing low–moderate $p185^{HER2/neu}$ (c) SK-BR-3 and T6-17 (NIH3T3 cells stably transfected with $p185^{HER2/neu}$, provided by J. Pierce, National

RESEARCH ARTICLES

Cancer Institute) cells (high concentration of $p185^{HER2/neu}$). NE91 murine fibroblasts expressing human EGFR have been described[45]. These cells were cultured and maintained in Dulbecco's modified Eagle's medium (DMEM) containing: 10% fetal bovine serum (FBS), 1% L-glutamine, and 1% penicillin/streptomycin at 37°C, 95% humidity, and 5% CO_2.

Cell proliferation. Proliferation was measured by standard MTT assay[38]. Cell lines were plated in 96-well plates (4,000 cells/well) in DMEM–10% FBS with indicated amount of AHNP or irrelevant CD4.M3, and were incubated for 24 h. Then MTT was given to the cells for 4 h. Cells were lysed in 50% SDS–20% DMSO and kept at 37°C overnight. Proliferation was assessed by taking optical density readings at 600 nm, using an ELISA reader. The number of cells used in these assays was determined to be within the linear range for this cell type.

Anchorage-independent growth. For the focus formation assay, 10^3 T6-17 cells were plated with 2×10^3 NR6 cells onto a 60 mm dish in DMEM medium with 2% FBS. Media, with or without antibodies or mimetics, were changed every three days. Fourteen days after plating, foci were scored after cells were fixed with 10% formalin and stained with hematoxylin. All experiments were done in triplicate and two or three independent studies were done. The next day, colonies were counted using an Alpha-imager system (Alpha Innotech, San Leandro, CA) for automatic counting. Large colonies were determined by automatic scaling for colonies >3 mm².

Apoptosis estimation by morphology and flow cytometry. For morphologic analysis, 30,000 cells were allowed to attach to coverslips overnight in six-well plates. Cells were incubated with 25 μg/ml of AHNP or CD4.M3 (an irrelevant peptide mimetic of volume/size equivalent molecular mass) for 24 h before γ-irradiation. γ-Irradiation (10 Gy) was applied and cells were incubated at 37°C for the indicated time periods. Nuclear morphology characteristic of apoptosis was assessed following staining with DAPI (4,6-diamidino-2-phenylindole) at the following time points after irradiation: 12, 24, 48, and 72 h. Statistical significance of the data was determined using Student's *t*-test, as previously used. For flow cytometry analysis, 200,000 cells were plated onto six-well dishes and allowed to attach overnight. Cells were then incubated with 25 μg/ml of AHNP, or irrelevant mimetic CD4/M3, for 2 h, and the indicated amount of doxorubicin was then added.

In vivo studies. NCr homozygous athymic (nude) mice (six to eight weeks-old) were purchased from the National Cancer Institute. An aliquot of 2×10^6 T6-17 cells were suspended in 200 μl of PBS and injected subdermally in the right thigh of each animals. Six days after tumor xenograft, tumors reached ~200–230 mm³ in volume. Animals were regrouped into four treatment groups: control, AHNP alone, doxorubicin alone, and AHNP in combination with doxorubicin. At day 6 and again at day 20, 100 μg of doxorubicin were given. Anti-HER 2/neu peptide was administered (200 μg) intraperitoneally three times a week from day 6 after tumor xenograft. Animals were maintained in accordance with guidelines of the Institutional Animal Care and Use Committee (IACUC) of the University of Pennsylvania. Tumor growth was monitored three times weekly for four weeks. Tumor volume was calculated by the formula: $\pi/6 \times$ (larger diameter) $\times$ (smaller diameter)³.

Acknowledgments

This work was supported by grants awarded to M.I.G. from the Abramson Cancer Institute, National Cancer Institute, NIH, and the US Army.

1. Slamon, D.J. et al. Human breast cancer: correlation of relapse and survival with amplification of the HER-2/neu oncogene. *Science* 235, 177–182 (1987).
2. Coussen, L.A. et al. Expression pattern of the *neu* (NGL) gene-encoded growth factor receptor protein (p185neu) in normal and transformed epithelial tissues of the digestive tract. *Oncogene* 4, 81–88 (1989).
3. Drebin, J.A., Link, V.C., Stern, D.F., Weinberg, R.A. & Greene, M.I. Development of monoclonal antibodies reactive with the product of the *neu* oncogene. *Symp. Fund. Cancer Res.* 38, 277–289 (1986).
4. Drebin, J.A., Link, V.C. & Greene, M.I. Monoclonal antibodies specific for the *neu* oncogene product directly mediate anti-tumor effects in vivo. *Oncogene* 2, 387–394 (1988).
5. Baselga, J., Norton, L., Albanell, J., Kim, Y.M. & Mendelsohn, J. Recombinant humanized anti-HER2 antibody (Herceptin) enhances the antitumor activity of paclitaxel and doxorubicin against HER2/neu overexpressing human breast cancer xenografts. *Cancer Res.* 58, 2825–2831 (1998).
6. Carter, P. et al. Humanization of an anti-p185HER2 antibody for human cancer therapy. *Proc. Natl. Acad. Sci. USA* 89, 4285–4289 (1992).
7. Fendly, B.M. et al. Characterization of murine monoclonal antibodies reactive to either the human epidermal growth factor receptor or HER2/neu gene product. *Cancer Res.* 50, 1550–1558 (1990).
8. Hudziak, R.M. et al. p185HER2 monoclonal antibody has antiproliferative effects in vitro and sensitizes human breast tumor cells to tumor necrosis factor. *Mol. Cell Biol.* 9, 1165–1172 (1989).
9. Drebin, J.A., Stern, D.F., Link, V.C., Weinberg, R.A. & Greene, M.I. Monoclonal antibodies identify a cell-surface antigen associated with an activated cellular oncogene. *Nature* 312, 545–548 (1984).
10. Drebin, J.A., Link, V.C., Weinberg, R.A. & Greene, M.I. Inhibition of tumor growth by a monoclonal antibody reactive with an oncogene-encoded tumor antigen. *Proc. Natl. Acad. Sci. USA* 83, 9129–9133 (1986).
11. Cho, M.J. & Juliano, R. Macromolecular versus small-molecule therapeutics: drug discovery, development and clinical considerations. *Trends Biotechnol.* 14, 153–158 (1996).
12. Hruby, V.J. Conformational and topographical considerations in the design of biologically active peptides. *Biopolymers* 33, 1073–1082 (1993).
13. Langston, S. Peptidomimetics and small molecule design. *Drug Discov. Today* 2, 254–256 (1997).
14. Qabar, M., Urban, J., Sia, C., Hruby, M. & Kahn, M. Pharmaceutical applications of peptidomimetics. *Lett. Pept. Sci.* 3, 25–30 (1996).
15. Murali, R. & Greene, M.I. Structure-based design of immunologically active therapeutic peptides. *Immunol. Res.* 17, 163–169 (1998).
16. Moore, G.J. Designing peptide mimetics. *Trends Pharmacol. Sci.* 15, 124–129 (1994).
17. KieberEmmons, T., Murali, R. & Greene, M.I. Therapeutic peptides and peptidomimetics. *Curr. Opin. Biotechnol.* 8, 435–441 (1997).
18. Saragovi, H.U. et al. Design and synthesis of a mimetic from an antibody complementarity-determining region. *Science* 253, 792–795 (1991).
19. Zhang, X. et al. Synthetic Cd4 exocyclic peptides antagonize Cd4 holoreceptor binding and T-cell activation. *Nat. Biotechnol.* 14, 472–475. (1996).
20. Takasaki, W., Kajino, Y., Kajino, K., Murali, R. & Greene, M.I. Structure-based design and characterization of exocyclic peptidomimetics that inhibit TNF alpha binding to its receptor. *Nat. Biotechnol.* 15, 1266–1270 (1997).
21. Chothia, C. & Lesk, A.M. Canonical structures for the hypervariable regions of immunoglobulins. *J. Mol. Biol.* 196, 901–917 (1987).
22. MacCallum, R.M., Martin, A.C. & Thornton, J.M. Antibody-antigen interactions: contact analysis and binding site topography. *J. Mol. Biol.* 262, 732–745 (1996).
23. Mariuzza, R.A., Phillips, S.E. & Poljak, R.J. The structural basis of antigen-antibody recognition. *Annu. Rev. Biophys. Biophys. Chem.* 16, 139–159 (1987).
24. Bruck, C. et al. Nucleic acid sequence of an internal image-bearing monoclonal anti-idiotype and its comparison to the sequence of the external antigen. *Proc. Natl. Acad. Sci. USA* 83, 6578–6582 (1986).
25. Eigenbrot, C., Randal, M., Presta, L., Carter, P. & Kossiakoff, A.A. X-ray structures of the antigen-binding domains from three variants of humanized anti-p185HER2 antibody 4D5 and comparison with molecular modeling. *J. Mol. Biol.* 229, 969–995 (1993).
26. Eigenbrot, C. et al. X-ray structures of fragments from binding and nonbinding versions of a humanized anti-CD18 antibody: structural indications of the key role of VH residues 59 to 65. *Proteins* 18, 49–62 (1994).
27. Zhang, H. et al. Pathobiological features of shared antigenic epitopes and biological functions of distinct and humanized anti-p185her2/neu monoclonal antibodies. *Exp. Mol. Pathol.* 67, 15–25 (1999).
28. Zheng, X. et al. Synthetic Cd4 exocyclics inhibit binding of human-immunodeficiency-virus type-1 envelope to Cd4 and virus-replication in T-lymphocytes. *Nat. Biotechnol.* 15, 150–154. (1997).
29. Ader, A.E.P., Hermkens, P.H.H., Linders, J.T.M., Ottenheijm, H.C.J. & van Staveren, C.J. Case histories of peptidomimetics: progression from peptides to drugs. *Recl. Trav. Chim. Pays-Bas.* 113, 63–78 (1994).
30. Akamatsu, M. et al. Potent inhibition of protein-tyrosine phosphatase by phosphotyrosine-mimic containing cyclic peptides. *Bioorg. Med. Chem.* 5, 157–163 (1997).
31. Graciani, N.R., Tseng, K.Y., McCutchen, S.L. & Kelly, J.W. Amino acids that specify structure through hydrophobic clustering and histidine-aromatic interactions lead to biologically active peptidomimetics. *Bioorg. Med. Chem.* 2, 999–1006 (1994).
32. McDonnell, J.M., Fushman, D., Cahill, S.M., Sutton, B.J. & Cowburn, D. Solution structures of Fc epsilon RI alpha-chain mimics: a beta-hairpin peptide and its retroenantiomer. *J. Am. Chem. Soc.* 119, 5321–5328 (1997).
33. Ylatluoss, I. et al. Phosphinic peptides, the first potent inhibitors of enkelin, behave as extremely slow-binding inhibitors. *Biochem. J.* 331, 375–379 (1998).
34. Benveniste, M. & Mayer, M.L. Structure-activity analysis of binding kinetics for NMDA receptor competitive antagonists: the influence of conformational restriction. *Br. J. Pharmacol.* 104, 207–221 (1991).
35. Moosmayer, D. et al. Characterization of different soluble TNF receptor (TNFR80) derivatives: positive influence of the intracellular domain on receptor/ligand interaction and TNF neutralization capacity. *J. Interf. Cytok. Res.* 16, 471–477 (1996).
36. Drebin, J.A., Link, V.C., Stern, D.F., Weinberg, R.A. & Greene, M.I. Down-modulation of an oncogene protein product and reversion of the transformed phenotype by monoclonal antibodies. *Cell* 41, 697–706 (1985).
37. Qian, X. et al. Identification of p185neu sequences required for monoclonal antibody- or ligand-mediated receptor signal attenuation. *DNA Cell Biol.* 16, 1395–1405 (1997).
38. Hansen, M.B., Nielsen, S.E. & Berg, K. Re-examination and further development of a precise and rapid dye method for measuring cell growth/cell kill. *J. Immunol. Methods* 119, 203–210 (1989).
39. Shepard, H.M. et al. Monoclonal antibody therapy of human cancer: taking the HER2 protooncogene to the clinic. [Review]. *J. Clin. Immunol.* 11, 117–127 (1991).
40. O'Rourke, D.M. et al. Conversion of a radioresistant phenotype to a more sensitive one by disabling erbB receptor signaling in human cancer cells. *Proc. Natl. Acad. Sci. USA* 95, 10842–10847 (1998).
41. Waldman, T. et al. Cell-cycle arrest versus cell death in cancer therapy. *Nat. Med.* 3, 1034–1036 (1997).
42. Katsumata, M. et al. Prevention of breast tumour development in vivo by down-regulation of the p185neu receptor. *Nat. Med.* 1, 644–648 (1995).
43. Qian, X., Dougall, W.C., Hellman, M.E. & Greene, M.I. Kinase-deficient neu proteins suppress epidermal growth factor receptor function and abolish cell transformation. *Oncogene* 9, 1507–1514 (1994).